Theoretical Prediction on the Thermal Stability of Cyclic Ozone and Strong Oxygen Tunneling

Jien-Lian Chen and Wei-Ping Hu

Department of Chemistry and Biochemistry, National Chung Cheng University

Chia-Yi, Taiwan 621

E-mail: chewph@ccu.edu.tw

Fax: 886-5-272-1040

5 Tables, 6 Figures, 26 pages, References.

Submitted to *Journal of the American Chemical Society* as supporting information, September, 2011.

I. Calculated geometries and Born-Oppenheimer energy.

Cyclic-ozone

Method/basis set : UB3LYP/cc-pVTZ
geometry :
O –0.0000520873,0., –0.0000894511
O –0.0000520873,0.,1.4315293679
O 1.2397661785,0.,0.7157199584
energy :
–225.453557 hartrees

Method/basis set : UMP2/aug-cc-pVTZ
geometry :
O –0.0073395152, 0., –0.0127116465
O –0.0073395152, 0. ,1.4441515633
O 1.2543410343, 0. ,0.7157199584
energy :
–225.080882 hartrees

Method/basis set : UCCSD(T)/aug-cc-pVTZ
geometry :
O
O 1 1.4472
O 1 1.4472 2 60.0
energy :
UCCSD(T)/aug-cc-pVTZ : –225.107243 hartrees
UCCSD(T)/aug-cc-pVQZ (SP) : –225.163573 hartrees

Method/basis set : CASSCF(18,12)/aug-cc-pVTZ
geometry :
O
O 1 1.457
O 1 1.457 2 60.0
energy :
–224.524827 hartrees

Method/basis set : MRCISD+Q(18,12)/aug-cc-pVTZ
geometry :
O
O 1 1.449
O 1 1.449 2 60.0
energy :
MRCISD+Q(18,12)/aug-cc-pVTZ : -225.100027 hartrees
MRCISD+Q(18,12)/aug-cc-pVQZ (SP) : -225.154468 hartrees

Open-ozone
Method/basis set : UB3LYP/cc-pVTZ
geometry :
O 0.0000245729,0., –0.0010889014
O –0.000995292,0.,1.2553415331
O 1.1061271558,0.,1.8493940245
energy :
–225.499071 hartrees

Method/basis set : UMP2/aug-cc-pVTZ
geometry :
O 0.0006018431, 0. , –0.0186077523
O –0.0172761773, 0., 1.2650732248
O 1.1218307709, 0., 1.8571811837
energy :
–225.139360 hartrees

Method/basis set : UCCSD(T)/aug-cc-pVTZ
geometry :
O
O 1 1.2766
O 1 1.2766 2 117.0
energy :
UCCSD(T)/aug-cc-pVTZ : –225.153478 hartrees
UCCSD(T)/aug-cc-pVQZ (SP) : –225.210614 hartrees

Method/basis set : CASSCF(18,12)/aug-cc-pVTZ
geometry :
O
O 1 1.291
O 1 1.291 2 116.7
energy :
–224.5732578 hartrees

Method/basis set : MRCISD+Q(18,12)/aug-cc-pVTZ
geometry :
O
O 1 1.282
O 1 1.282 2 116.7
energy :
MRCISD+Q(18,12)/aug-cc-pVTZ –225.148909 hartrees
MRCISD+Q(18,12)/aug-cc-pVQZ (SP) : –225.204595 hartrees

Transition state
Method/basis set : UMP2/aug-cc-pVTZ
geometry :
O 0.,0.,0.
O 0.,0.,1.366
O 1.3527061819,0.,0.1901104559
energy :
–225.042405 hartrees

Method/basis set : UB3LYP/cc-pVTZ
geometry :
O –0.0004846618,0., –0.0002615119
O 0.0001265962,0.,1.3806210828
O 1.3499254958,0.,1.0892792825
energy :
–225.426211 hartrees

Method/basis set : UCCSD(T)/aug-cc-pVTZ
geometry :
O
O 1 1.395
O 1 1.395 2 80.2
energy :
UCCSD(T)/aug-cc-pVTZ : –225.076466 hartrees
UCCSD(T)/aug-cc-pVQZ (SP) : –225.132072 hartrees

Method/basis set : CASSCF(18,12)/aug-cc-pVTZ
geometry :
O
O 1 1.427
O 1 1.427 2 83.8
energy :
–224.488596 hartrees

Method/basis set : MRCISD+Q(18,12)/aug-cc-pVTZ
geometry :
O
O 1 1.410
O 1 1.410 2 84.0
energy :
MRCISD+Q(18,12)/aug-cc-pVTZ : –225.059802 hartrees
MRCISD+Q(18,12)/aug-cc-pVQZ (SP) : –225.113274 hartrees

CP1
Method/basis set : CASSCF(18,12)/aug-cc-pVTZ
geometry :
O
O 1 1.416
O 1 1.416 2 80.3
energy :

–224.494894 hartrees

Method/basis set : MRCISD+Q(18,12)/aug-cc-pVTZ
geometry :
O
O 1 1.416
O 1 1.416 2 79.7
energy :
MRCISD+Q(18,12)/aug-cc-pVTZ : –225.068348 hartrees
MRCISD+Q(18,12)/aug-cc-pVQZ (SP) : –225.120770 hartrees

CP2
Method/basis set : CASSCF(18,12)/aug-cc-pVTZ
geometry :
O
O 1 1.406
O 1 1.406 2 89.2
energy :
–224.514163 hartrees

Method/basis set : MRCISD+Q(18,12)/aug-cc-pVTZ
geometry :
O
O 1 1.401
O 1 1.401 2 89.6
energy :
MRCISD+Q(18,12)/aug-cc-pVTZ : –225.088732 hartrees
MRCISD+Q(18,12)/aug-cc-pVQZ (SP) : –225.141447 hartrees

II. Concise Description of the Theoretical Methods

Variational Transition State Theory (VTST)

VTST is the generalized version of the conventional transition state theory where the position of the transition state (or reaction bottleneck) can be variationally positioned under various constraints so as to minimize the one-way flux of the reaction from the reactants to the products.[S1–S3] The version applied in the current study is the canonical variational theory (CVT) where a single variational transition state is located on the reaction path at a particular temperature.[S2–S3] The reaction path on the PES needs to be calculated starting from the transition state towards the reactant and the product. This is usually achieved by using an efficient integrator, such as the Page-McIver algorithm mentioned in the text. The integrator requires the energy gradients and hessians information to "follow" the reaction path, so usually relatively small gradient- and hessian-step sizes need to be specified.

Small-curvature tunneling method (SCT) :

The SCT method is based on the centrifugal-dominant small-curvature semiclassical ground-state (CD-SCSAG) method.[S4] In this method, the tunneling path is assumed to follow the turning points obtained from the perpendicular vibrational motion of the molecular species on the concave side of the reaction path. The transmission coefficients are then obtained from the Boltzmann averages of the tunneling probabilities at various energies.

Large-curvature tunneling method (LCT):

The LCT calculations are base on the straight tunneling path connecting the molecular species on the reactant and the product side with the same energies.[S4–S6] The transmission coefficients are then obtained from the Boltzmann averages of the tunneling probabilities at various energies.

Microcanonical optimized multidimensional tunneling method (μOMT) :

The μOMT tunneling probability at each energy is determined by the larger of the SCF and LCT tunneling probabilities.[S6] The transmission coefficients are then obtained from the Boltzmann averages. In the above tunneling methods, the movements of all atoms contributed to the calculation of the tunneling path and tunneling probabilities. Thus, they are sometimes called multi-dimensional tunneling (MT) methods.

Quantized-Reactant-State Tunneling (QRST) :

In the QRST calculation, the discrete vibrational energy levels at the reactant side are used in the tunneling calculation.[S7,S8] (The traditional semiclassical tunneling methods assume continuous energy levels.) The energy levels in principle can be determined from the potential energy curve on the reactant side. However, they are often approximated by the harmonic energy levels of a selected vibrational mode of the reactant that resembles the reaction-path mode.

Dual-Level Dynamics :

The conventional direct dynamics calculation is based on a single-level potential energy surface (PES). The cost of many (thousands or more) electronic structure calculations prevent one from using a very high-level theory, and thus the accuracy of the dynamics calculation suffers from the low quality of the PES data. Dual-level dynamics methods were designed to overcome this difficulty at affordable cost. In dual-level VTST method, the PES information on the stationary points (reactant, product, transition state) is calculated using a highest possible theory (the high level, MRCISD+Q/aug-cc-pVQZ in the current study). The global PES data along the reaction path are calculated using a qualitatively correct theory (the low-level, UB3LYP/cc-pVTZ in the current study). Then interpolated correction methods are applied to correct the reaction-path data between the stationary points based on the differences between the high- and low-level data.[S9]

SIL-1 Scheme:

The SIL-1 scheme[S10] is a popular way to perform the dual-level VTST calculation that also gives a reasonable estimate of the barrier width. In this scheme, an intermediate level single-point calculation (MRCISD+Q/aug-cc-pVTZ in the current study) is performed along the low-level reaction path to estimate a reliable barrier width. Then the range parameters in the interpolated correction functions for the energies are adjusted such that the corrected barrier width agrees with the width obtained from the intermediate calculation. This is especially important for tunneling calculation.

Multi-Reference Configuration Interaction Method (MRCI) :

Many chemical systems, including ozone, can only be appropriately modeled with multi-configurational electronic theory, such as the MCSCF method. While the MCSCF theory properly includes the static correlation energies of these systems, quantitative results also require accurate treatment on the dynamic correlation

energies. In MRCI method,[S11] the reference wavefunction is usually obtained from a previously converged MCSCF calculation (full-valence complete-active space SCF in the current study). The most important configurations are then subjected to configuration interaction expansion to include the dynamic correlation energies. Usually the CI expansion is restricted to single (S) and double (D) excitations, and the contribution from quadruple excitations was estimated semiclassically, such as using Davidson's correction formula.[S12] The resulting method (called MRCISD+Q), when used with a large basis set, is of very good quality even for very difficult cases, such as the current system. The expected accuracy on the relative energies of the electronic ground state for the current system is ~1 kcal/mol using the MRCISD+Q/aug-cc-pVQZ theory.

III. Sample Input File (Gaussrate 8.2)

VTST/MT input files for cyclic-ozone→ open-ozone
Level: dual-level CVT/μOMT–QRST

```
unit fu5 (main input file)
{
*General

 TITLE
 cyclic-ozone -> open-ozone
 Calculation of ALL
 END

  ATOMS
    1 O
    2 O
    3 O
  END

  NOSUPERMOL

ICOPT
  energy seckart
  freq   icl
  correct on
  both
END

*OPTIMIZATION

  OPTMIN  OHOOK
  OPTTS   OHOOK

*SECOND

  HESSCAL HHOOK

*REACT1

STATUS 6
 # Geometry in a.u.
  GEOM
    1         0.00000000      1.56192412      0.00000000
    2         1.35266597     -0.78096206      0.00000000
    3        -1.35266597     -0.78096206      0.00000000
  END
 # Energy in a.u.
  ENERGY   -225.4535570715000
 # Frequencies in a.u.
  VIB
    0.5507772659E-02   0.3913002586E-02   0.3913002585E-02
  END

  SPECIES  NONLINRP
```

```
# end of react1 section

*PROD1

STATUS 6
 # Geometry in a.u.
  GEOM
    1         0.00000000      2.03694297     -0.40660320
    2         0.00000000      0.00000000      0.81320641
    3         0.00000000     -2.03694297     -0.40660320
  END
 # Energy in a.u.
  ENERGY   -225.4990711018029
 # Frequencies in a.u.
  VIB
    0.5697992138E-02    0.5429700388E-02    0.3395245215E-02
  END

  SPECIES  NONLINRP

# end of prod1 section

*START

STATUS 4
 # Geometry in a.u.
  GEOM
    1         0.00000000     -1.63945116     -0.67666035
    2         0.00000000      0.00000000      1.35332069
    3         0.00000000      1.63945116     -0.67666035
  END
 # Energy in a.u.
  ENERGY   -225.4262108937410
 # Frequencies in a.u.
HESSIAN
-0.1342891450E-32
-0.1303915474E-16    0.5162259997E-03
0.1099428794E-16    0.2643100204E+00    0.1049500773E+00
0.1087275884E-32    0.1561739602E-16   -0.2650996179E-17
0.1026443644E-32
0.8380436285E-25   -0.8593606582E-01   -0.1064066977E+00
0.1052413286E-16
0.1718721316E+00
-0.2198857597E-16   -0.4222133430E+00   -0.7814656307E-01
-0.7729069905E-17
0.4852940537E-11    0.1562931261E+00
0.2550405381E-33   -0.2578241303E-17   -0.8343291796E-17
-0.2113683023E-32
-0.1052413291E-16    0.2971764591E-16    0.1858677480E-32
 0.1303915465E-16    0.8541983982E-01   -0.1579033226E+00
-0.2614152889E-16
-0.8593606581E-01    0.4222133430E+00    0.1310237421E-16
0.5162259838E-03
0.1099428804E-16    0.1579033226E+00   -0.2680351426E-01
0.1038006608E-16
0.1064066977E+00   -0.7814656306E-01   -0.2137435411E-16
-0.2643100204E+00
 0.1049500773E+00
END

  SPECIES  NONLINTS
```

```
# end of start section

*PATH

 SCALEMASS  1.00

 INTMU   3
 SSTEP   0.01
 INH    5

 SRANGE
   SLP   3.2
   SLM  -1.9
 END

 RPM    PageM

 SIGN   reactant

 COORD   CURV3
 INTDEF
 1-2 1-3 2-3
 1-2-3 2-3-1
 END

PRPATH
    XMOL
END

# end of path section
*TUNNEL

  LCT

  QRST
   harmonic
   srw  -1.9
   mode 3
  END

# end of tunnel section

*RATE

  FORWARDK

  SIGMAF 3

   CVT

  TEMP
25
50
75
100
125
150
175
200
250
```

```
300
400
500
END
}
```

unit fu50 (The input file of dual-level dynamics)

```
{
*VTSTIC         # unit fu50 input file

 MEPTYPER  ONE   # one reactants
 MEPTYPEP  ONE    # one products

 ENESAD  21.12  # the classical barrier height in kcal/mol

 ENERXN  -31.46  #the exerogicity in kcal/mol

# NOFREQMAT       # No frequency matching is needed for 0IVTST
calculations


 DETMI
 2.4292E+15          # Det I of reactant
 0
 2.9732E+15          # Det I of saddle point
 1.8954E+15          # Det I of product
 0
 END

 UNITMI   au             #from gaussian output

 RANGEIC
    BR   7.4
    BP   50.0
 END
 PCINFO
   SPC   3.2
 END
 RCINFO
   SRC -1.9
 END

 FREQIMAG 1055.24  # the imaginary frequency of saddle point in cm-1 UB3LYP
/aug-cc-pVTZ
#the frequency of UB3LYP/aug-cc-pVTZ

 RCFREQA
 1208.82 858.80 858.80
 END

 PCFREQA
 1250.56 1191.68 745.17
 END

 SADFREQ
 1166.26 802.24
 END
}
```

Table S1. Calculated Harmonic Vibrational Frequencies of cyclic ozone, open ozone, and transition state (cm^{-1}).

	$^{16}O^{16}O^{16}O$	$^{18}O^{16}O^{16}O$	$^{16}O^{18}O^{16}O$	$^{18}O^{18}O^{16}O$	$^{18}O^{16}O^{18}O$	$^{18}O^{18}O^{18}O$	exp[a]
				cyclic-ozone			
symmetric stretching	1209	1187	1187	1164	1164	1139	
anti-symmetric stretching	859	843	843	826	826	810	
Bending	859	841	841	825	825	810	
				open-zone			
symmetric stretching	1251	1236	1218	1203	1213	1179	1103
anti-symmetric stretching	1192	1174	1151	1133	1165	1123	1042
Bending	745	728	732	719	710	702	701
				transition state			
symmetric stretching	1166	1147	1139	1120	1127	1099	
anti-symmetric stretching	802	789	780	769	777	756	
Bending	1055 *i*	1033 *i*	1039 *i*	1017 *i*	1010 *i*	994 *i*	

[a] from ref S13

Table S2. Calculated Rate Constants[a] (s^{-1}) by TST

T (K)	$^{16}O^{16}O^{16}O$	$^{18}O^{16}O^{16}O$	$^{16}O^{18}O^{16}O$	$^{18}O^{18}O^{16}O$	$^{18}O^{16}O^{18}O$	$^{18}O^{18}O^{18}O$
25	3.83(−161) [b]	9.97(−162)	1.33(−161)	3.42(−162)	1.03(−161)	7.88(−162)
50	1.63(−74)	4.78(−75)	7.84(−75)	2.82(−75)	6.88(−75)	7.38(−75)
75	1.46(−45)	4.45(−46)	7.83(−46)	3.14(−46)	7.16(−46)	8.60(−46)
100	4.74(−31)	1.48(−31)	2.69(−31)	1.14(−31)	2.51(−31)	3.19(−31)
125	2.55(−22)	8.04(−23)	1.49(−22)	6.55(−23)	1.41(−22)	1.86(−22)
150	1.74(−16)	5.53(−17)	1.04(−16)	4.68(−17)	9.93(−17)	1.34(−16)
175	2.62(−12)	8.38(−13)	1.59(−12)	7.26(−13)	1.53(−12)	2.09(−12)
200	3.62(−9)	1.16(−9)	2.23(−9)	1.03(−9)	2.15(−9)	2.97(−9)
250	9.34(−5)	3.02(−5)	5.85(−5)	2.74(−5)	5.67(−5)	7.96(−5)
300	8.40(−2)	2.73(−2)	5.31(−2)	2.52(−2)	5.17(−2)	7.34(−2)
400	4.33(2)	1.41(2)	2.77(2)	1.33(2)	2.71(2)	3.89(2)
500	7.53(4)	2.46(4)	4.85(4)	2.34(4)	4.75(4)	6.87(4)

[a] Symmetry numbers used for $^{16}O^{16}O^{16}O$、$^{18}O^{16}O^{16}O$、$^{16}O^{18}O^{16}O$、$^{18}O^{18}O^{168}O$、$^{18}O^{16}O^{18}O$、$^{18}O^{18}O^{18}O$ reactions are 3, 2, 1, 2, 1, and 3 respectively.

[b] 3.83(−161) means 3.78×10^{-161}

Table S3. Calculated Rate Constants[a] (s^{-1}) by CVT/μOMT

T (K)	$^{16}O^{16}O^{16}O$	$^{18}O^{16}O^{16}O$	$^{16}O^{18}O^{16}O$	$^{18}O^{18}O^{16}O$	$^{18}O^{16}O^{18}O$	$^{18}O^{18}O^{18}O$
25	2.46(–4) [b]	3.28(–5)	4.68(–5)	1.46(–5)	3.56(–5)	2.73(–5)
50	6.03(–4)	8.03(–5)	1.15(–4)	3.62(–5)	8.79(–5)	6.80(–5)
75	1.15(–3)	1.54(–4)	2.20(–4)	7.06(–5)	1.70(–4)	1.34(–4)
100	2.07(–3)	2.78(–4)	4.01(–4)	1.31(–4)	3.15(–4)	2.52(–4)
125	3.82(–3)	5.18(–4)	7.53(–4)	2.56(–4)	6.05(–4)	5.04(–4)
150	7.73(–3)	1.06(–3)	1.56(–3)	5.69(–4)	1.32(–3)	1.17(–3)
175	1.83(–2)	2.56(–3)	3.85(–3)	1.55(–3)	3.48(–3)	3.46(–3)
200	5.28(–2)	7.62(–3)	1.17(–2)	5.39(–3)	1.16(–2)	1.33(–2)
250	7.39(–1)	1.16(–1)	1.86(–1)	1.07(–1)	2.17(–1)	3.14(–1)
300	1.41(1)	2.58(0)	4.34(0)	2.66(0)	5.27(0)	8.43(0)
400	3.60(3)	8.99(2)	1.65(3)	9.25(2)	1.84(3)	2.92(3)
500	2.43(5)	6.91(4)	1.32(5)	6.94(4)	1.39(5)	2.14(5)

[a] Symmetry numbers used for $^{16}O^{16}O^{16}O$、$^{18}O^{16}O^{16}O$、$^{16}O^{18}O^{16}O$、$^{18}O^{18}O^{16}O$、$^{18}O^{16}O^{18}O$、$^{18}O^{18}O^{18}O$ reactions are 3, 2, 1, 2, 1, and 3 respectively.

[b] 2.46(–4) means 2.46×10^{-4}

Table S4. Calculated KIE ($^{16}O/^{18}O$) by CVT/μOMT

T (K)	KIE1	KIE2	KIE3
25	3.09	4.89	9.00
50	3.09	4.85	8.85
75	3.07	4.77	8.61
100	3.05	4.65	8.21
125	3.01	4.44	7.58
150	2.94	4.10	6.59
175	2.85	3.63	5.28
200	2.74	3.11	3.98
250	2.45	2.28	2.36
300	2.04	1.78	1.67
400	1.41	1.30	1.23
500	1.21	1.17	1.13

Table S5. Calculated excitation energies of cyclic ozone at MRCISD+Q/aug-cc-pVTZ level and transition dipole moments at MCSCF/aug-cc-pVTZ level. (all relative to the $1A_1$ state)

	A_1	A_2	B_1	B_2
ground state	0.00[a]	4.00 (0.00000)[b]	7.90 (0.02496)	4.00 (0.00043)
first excited state	7.97 (0.02466)	5.28 (0.00000)	8.67 (0.01191)	5.19 (0.02244)
second excited state	8.65 (0.00157)	5.30 (0.00000)	7.36 (0.09821)	5.30 (0.11886)
third excited state	8.70 (0.00967)	8.94 (0.00000)	7.48 (0.00070)	10.61 (0.00063)

[a]Calculated excitation energies in eV

[b]Calculated absolute transition dipole moments in au.

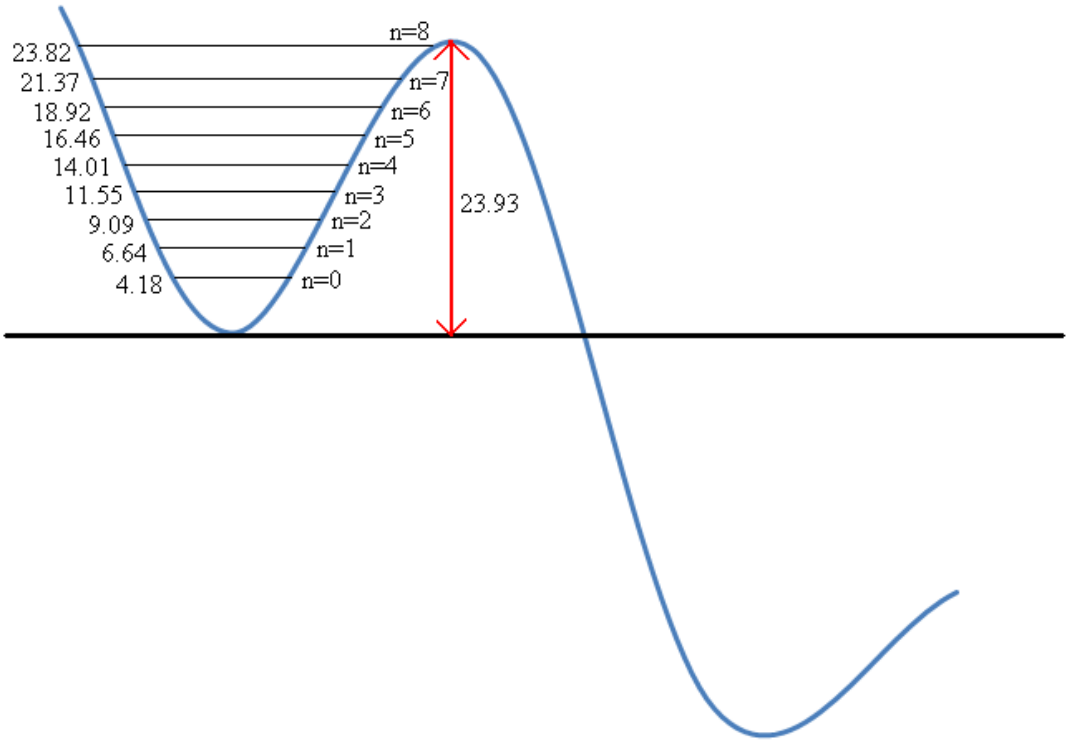

Figure S1. The reactant energy levels (kcal/mol) used in the QRST calculation for cyclic-$^{16}O^{16}O^{16}O$ → open-$^{16}O^{16}O^{16}O$. The zero of energy is the classical energy of the reactant, and the energy levels is the relative classical energies plus the vibrational zero-point energies along the reaction path.

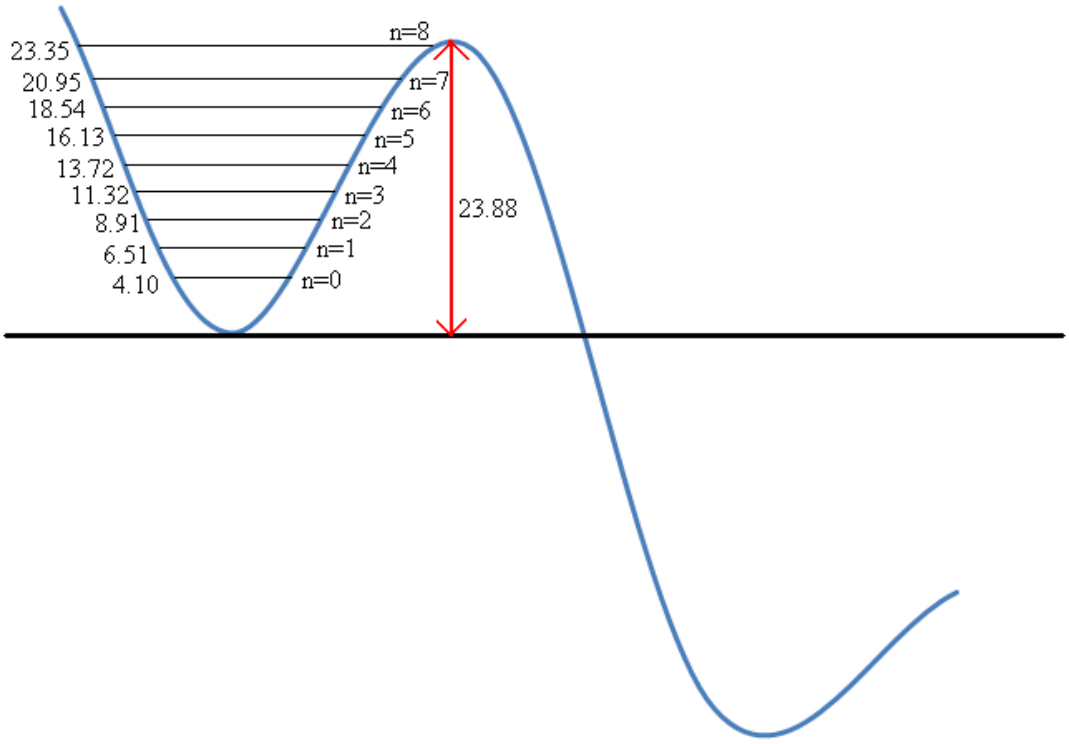

Figure S2. The reactant energy levels (kcal/mol) used in the QRST calculation for cyclic-$^{18}O^{16}O^{16}O$ → open-$^{18}O^{16}O^{16}O$. The zero of energy is the classical energy of the reactant, and the energy levels is the relative classical energies plus the vibrational zero-point energies along the reaction path.

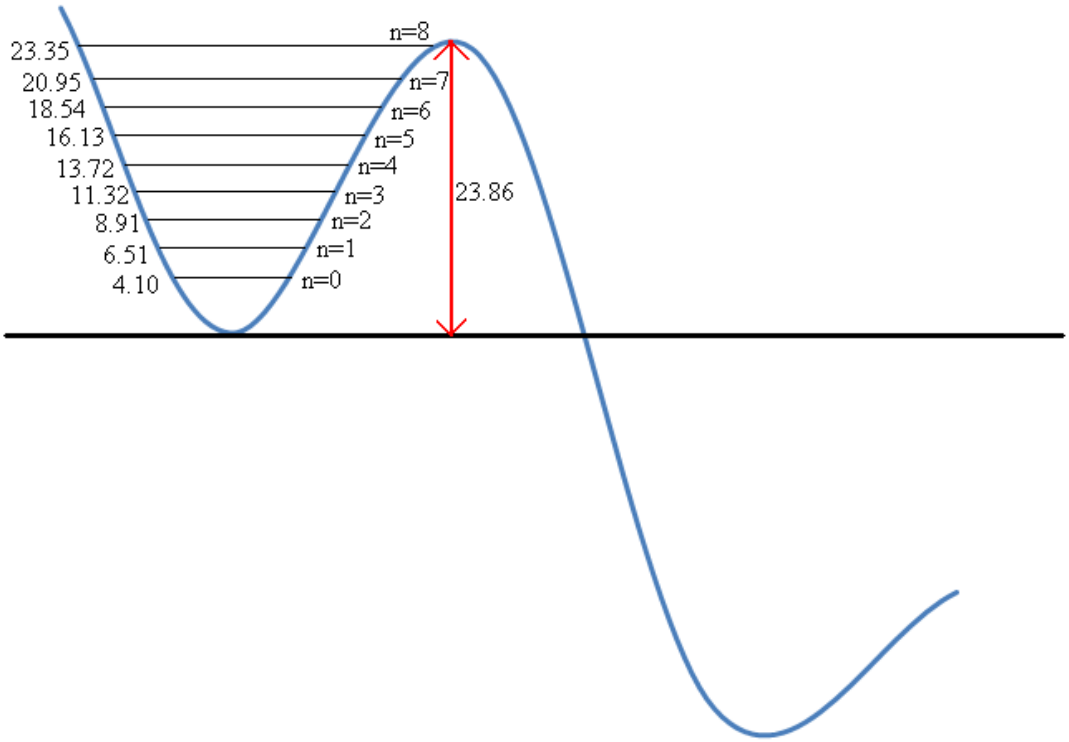

Figure S3. The reactant energy levels (kcal/mol) used in the QRST calculation for cyclic-$^{16}O^{18}O^{16}O$ → open-$^{16}O^{18}O^{16}O$. The zero of energy is the classical energy of the reactant, and the energy levels is the relative classical energies plus the vibrational zero-point energies along the reaction path.

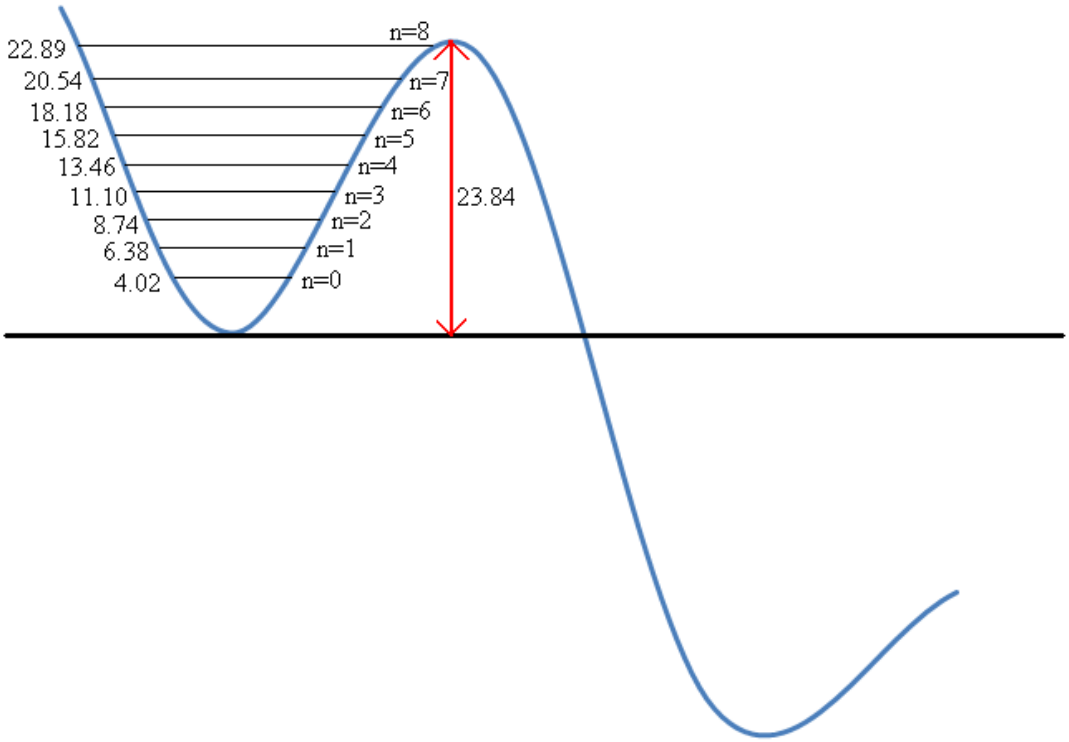

Figure S4 The reactant energy levels (kcal/mol) used in the QRST calculation for cyclic-$^{18}O^{16}O^{18}O$ → open-$^{18}O^{16}O^{18}O$. The zero of energy is the classical energy of the reactant, and the energy levels is the relative classical energies plus the vibrational zero-point energies along the reaction path.

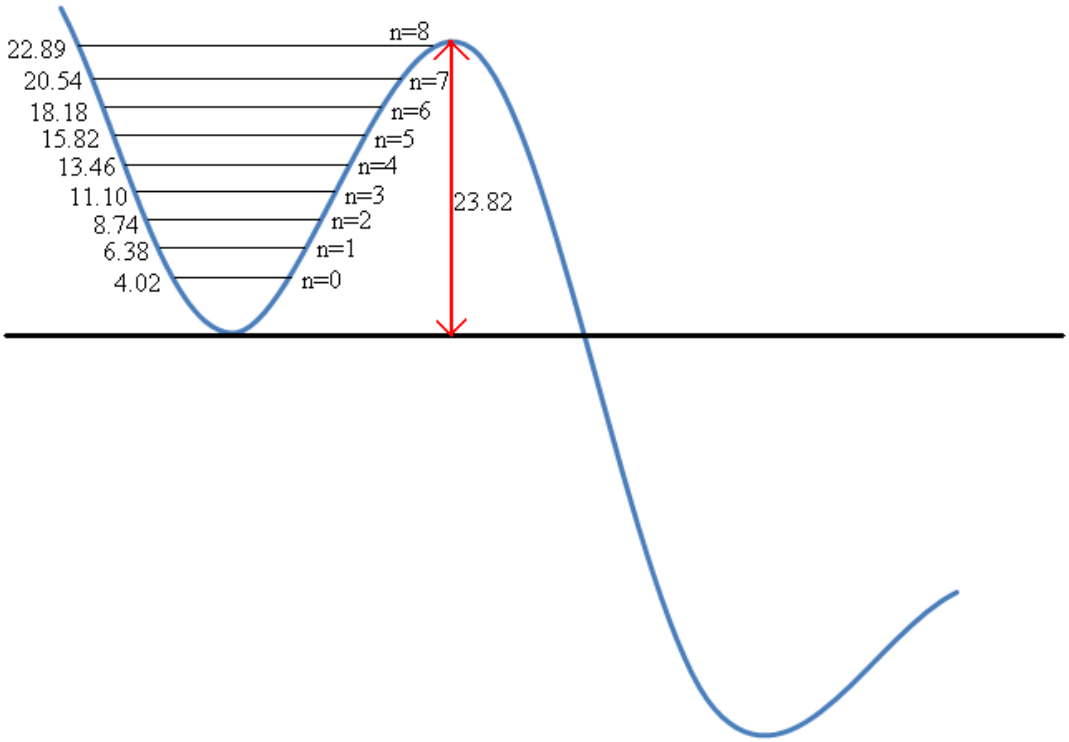

Figure S5 The reactant energy levels (kcal/mol) used in the QRST calculation for cyclic-$^{18}O^{18}O^{16}O$ → open-$^{18}O^{18}O^{16}O$. The zero of energy is the classical energy of the reactant, and the energy levels is the relative classical energies plus the vibrational zero-point energies along the reaction path.

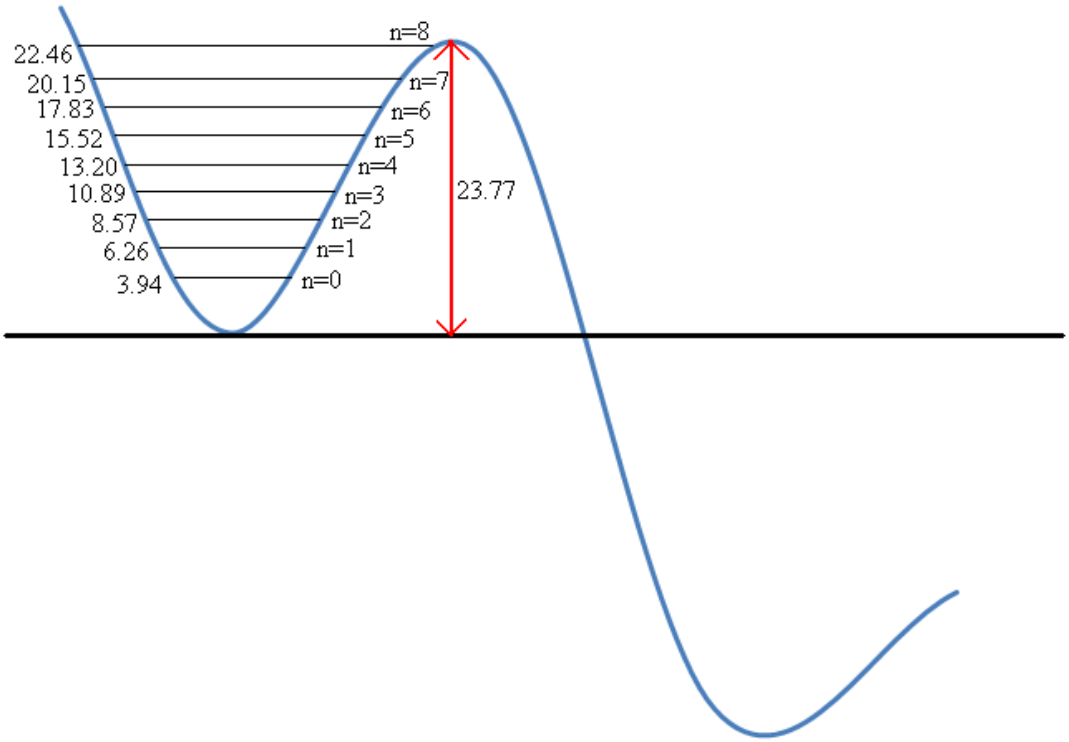

Figure S6 The reactant energy levels (kcal/mol) used in the QRST calculation for cyclic-$^{18}O^{18}O^{18}O$ → open-$^{18}O^{18}O^{18}O$. The zero of energy is the classical energy of the reactant, and the energy levels is the relative classical energies plus the vibrational zero-point energies along the reaction path.

References

S1. Truhlar, D. G.; Garrett, B. C. *Acc. Chem. Res.* **1980**, *13*, 440.

S2. Truhlar, D. G.; Isaacson, A. D.; Garrett, B. C. In *Theory of Chemical Reaction Dynamics*; Baer, M., Ed.; CRC Press: Boca Raton, FL, 1985; Vol. 4, p 65.

S3. Truhlar, D. G.; Garrett, B. C.; Klippenstein, S. J. *J. Phys. Chem.* **1996**, *100*, 12771.

S4. (a) Liu, Y.-P.; Lynch, G. C.; Truong, T. N.; Lu, D.-H.; Truhlar, D. G.; Garrett, B. C. *J. Am. Chem. Soc.* **1993***, 115,* 2408. (b) Lu, D.-H.; Truong, T. N.; Melissas, V. S.; Lynch, G. C.; Liu, Y.-P.; Garrett, B. C.; Steckler, R.; Isaacson, A. D.; Rai, S. N.; Hancock, G. C.; Lauderdale, J. G.; Joseph, T.; Truhlar, D. G. *Comput. Phys. Commun.* **1992**, *71*, 235.

S5. Truong, T. N.; Lu, D.-H.; Lynch, G. C.; Liu, Y.-P.; Melissas, V. S.; Gonzalez-Lafont, A.; Rai, S. N.; Steckler, R.; Garrett, B. C.; Joseph, T.; Truhlar, D. G. *Comput. Phys. Commun.* **1993**, *75*, 143.

S6. Liu, Y.-P.; Lu, D.-H.; Gonzalez-Lafont, A.; Truhlar, D. G.; Garrett, B. C. *J. Am. Chem. Soc.* **1993**, *115*, 7806.

S7. Wonchoba, S. E.; Hu, W.-P.; Truhlar, D. G. In *Theoretical and Computational Approaches to Interface Phenomena*; Sellers, H. L.,Golab, J. T., Eds.; Plenum Press: New York, 1994; p 1.

S8. Wonchoba, S. E.; Hu, W.-P.; Truhlar, D. G. *Phys. Rev. B* **1995**, *51*, 9985.

S9. Hu, W.-P.; Liu, Y.-P.; Truhlar, D. G. *J. Chem. Soc. Faraday Trans.* **1994**, *90*, 1715.

S10. Huang, C.-H.; You, R.-M.; Lian, P.-Y.; Hu, W.-P. *J. Phys. Chem. A* **2000**, *104,* 7200.

S11. Werner, H-J.; Knowles, P. J. *J. Chem. Phys.* **1988**, *89,* 5803.

S12. Langhoff, S. R.; Davidson, E. R. *Int. J. Quantum Chem.* **1974**, *8,* 61.

S13. Tyterev, V. G.; Tashkun, S.; Jensen, P.; Barbe, A.; Cours, T. *J. Mol. Spectrosc.* **1999** , *198*, 57.

Complete references of Ref. 44 and Ref. 47 in the main text

44. Gaussian 03, Revision E.01, Frisch, M. J.; Trucks, G. W.; Schlegel, H. B.; Scuseria, G. E.; Robb, M. A.; Cheeseman, J. R.; Montgomery, Jr., J. A.; Vreven, T.; Kudin, K. N.; Burant, J. C.; Millam, J. M.; Iyengar, S. S.; Tomasi, J.; Barone, V.; Mennucci, B.; Cossi, M.; Scalmani, G.; Rega, N.; Petersson, G. A.; Nakatsuji, H.; Hada, M.; Ehara, M.; Toyota, K.; Fukuda, R.; Hasegawa, J.; Ishida, M.; Nakajima, T.; Honda, Y.; Kitao, O.; Nakai, H.; Klene, M.; Li, X.; Knox, J. E.; Hratchian, H. P.; Cross, J. B.; Bakken, V.; Adamo, C.; Jaramillo, J.; Gomperts, R.; Stratmann, R. E.; Yazyev, O.; Austin, A. J.; Cammi, R.; Pomelli, C.; Ochterski, J. W.; Ayala, P. Y.; Morokuma, K.; Voth, G. A.; Salvador, P.; Dannenberg, J. J.; Zakrzewski, V. G.; Dapprich, S.; Daniels, A. D.; Strain, M. C.; Farkas, O.; Malick, D. K.; Rabuck, A. D.; Raghavachari, K.; Foresman, J. B.; Ortiz, J. V.; Cui, Q.; Baboul, A. G.; Clifford, S.; Cioslowski, J.; Stefanov, B. B.; Liu, G.; Liashenko, A.; Piskorz, P.; Komaromi, I.; Martin, R. L.; Fox, D. J.; Keith, T.; Al-Laham, M. A.; Peng, C. Y.; Nanayakkara, A.; Challacombe, M.; Gill, P. M. W.; Johnson, B.; Chen, W.; Wong, M. W.; Gonzalez, C.; and Pople, J. A.; Gaussian, Inc., Wallingford CT, 2004.

47. Chuang, Y.-Y.; Corchado, J. C.; Fast P. L.; Villa, J.; Hu,W.-P.; Liu, Y. P.;Lynch, G. C.;Nguyen, K. A.; Jackels, C. F.; Gu, M. Z.; Rossi, I.; Coitino, E. L.; Clayton, S.; Melissas, V. S.; Steckler, R.;Garrett, B. C.; Isaacson, A. D.; Truhlar, D. G. *Polyrate*-version 8.2; University of Minnesota: Minneapolis, MN, 1999.